The neuroprotection of hyperbaric oxygen therapy against traumatic brain injury via NF-κB/MAPKs-CXCL1 signaling pathway

Anqi Xia
Affiliated Hospital of Nantong University:Department of Rehabilitation Medicine
Huan Huang
Affiliated Hospital of Nantong University:Department of Rehabilitation Medicine
Wenjun You
Affiliated Hospital of Nantong University,the Second Peoples Hospital of Nantong:Department of geriatrics
Ying Liu
Affiliated Hospital of Nantong University:Department of pathology
Hongqin Wu
Affiliated Hospital of Nantong University:Department of Rehabilitation Medicine
Su Liu (327202278@qq.com)
Affliated Hospital of NanTong University

Research

Keywords: Hyperbaric oxygen, Traumatic brain injury, CXCL1, CXCR2

Posted Date: December 29th, 2020

DOI: https://doi.org/10.21203/rs.3.rs-135105/v1

Version of Record: A version of this preprint was published at Experimental Brain Research on October 23rd, 2021. See the published version at https://doi.org/10.1007/s00221-021-06249-8.

Abstract

Background

It is well known that hyperbaric oxygen (HBO) therapy achieves neuroprotective effects by suppressing or relieving neuroinflammatory responses. However, its underlying therapeutic mechanisms are not yet fully elucidated. Based on our previous studies, we further investigated whether HBO therapy exerts neuroprotective effects *in vivo* by regulating the NF-κB/ MAPKs-CXCL1 inflammatory pathway.

Methods

A rat model of traumatic brain injury (TBI) was established by controlled cortical impact (CCI). The cellular distribution of CXCL1 and CXCR2 was observed by double immunofluorescence labeling. The neurological function of TBI rats was assessed by modified neurological severity scores and Morris water maze methods. TUNEL staining was performed to observe apoptosis of neuronal cells in the injured cortical area. The changes in neural function, neuronal apoptosis, and expression of CXCL1, CXCR2, NF-κB, and MAPKs (ERK and JNK) were observed in TBI rats treated with CXCR2 antagonist, ERK, JNK, and NF-κB inhibitor or HBO therapy.

Results

The expression of CXCL1 and CXCR2 increased after TBI, and cell localization analysis revealed that CXCL1 was mainly expressed in astrocytes, while CXCR2 was mainly expressed in neurons. Increased apoptosis of cortical neurons in the injury area was also found after TBI. Reduced neuronal apoptosis with improved neurological function was observed after application of a CXCR2 antagonist. The expression of p-ERK, p-JNK and p-NF-κB increased after TBI, and application of ERK, JNK and NF-κB inhibitors decreased expression of CXCL1 and CXCR2 in rats. We further found that HBO therapy down-regulated the expression of p-ERK, p-JNK, p-NF-κB, CXCL1, and CXCR2, and reduced neuronal apoptosis, improved the neurological function of TBI rats, and ultimately alleviated the secondary injury.

Conclusions

CXCL1- CXCR2 mediates the interaction of activated astrocytes and neurons, exacerbating secondary injury after TBI. HBO therapy exerts neuroprotective effects by regulating the NF-κB/ MAPKs (JNK and ERK)- CXCL1 inflammatory pathway to control neuroinflammation after TBI, which provides the theoretical and experimental basis for the clinical application of HBO therapy in the treatment of TBI.

Introduction

The yearly incidence of traumatic brain injury (TBI) is estimated at 50 million cases worldwide, and thus TBI is a major global health challenge [1]. The high rates of TBI-associated morbidity and mortality in China, a large developing country, has become a major public health concern [2]. TBI includes primary and secondary injuries. Compared to primary injuries, secondary injuries last longer and are the focus of scientific research and clinical treatment for TBI. Secondary injuries include neuroinflammation, disruption of the blood-brain barrier, abnormal brain metabolism, and excitotoxicity. Neuroinflammation is a major pathogenic mechanism leading to secondary brain injuries following TBI. It has been reported in the literature that the expression of various inflammatory factors, such as IL-1β, CCL2, CXCL1, IFN-γ, TNF-α, IL-6, IL-1α, IL-10 and IL-8, is altered after TBI. These factors, involved in the molecular regulatory mechanisms of neuroinflammatory response, are classified into two major groups: pro-inflammatory and anti-inflammatory factors [3–6]. Moreover, it has been shown that neuroinflammation modulation may be a favorable option for the alleviation of secondary brain injuries and to ameliorate the outcome of TBI [7–9].

The use of hyperbaric oxygen (HBO) for the treatment of TBI has been controversial, mainly because of uncertainty of its efficacy, complications associated with HBO therapy, and the fact that the therapeutic mechanisms have not been completely clarified [10–13]. Numerous animal studies and clinical practice have demonstrated that HBO treatment can reduce secondary injury after TBI. In 2018, a neurosurgery clinical team from the University of Minnesota published a review on the treatment of acute TBI with HBO that collected and analyzed 30 clinical and animal research articles. Their results showed clear efficacy of HBO in the treatment of acute TBI [14]. Preliminary studies of our group also confirmed that HBO treatment can reduce secondary injury after TBI, and its mechanism of action may be related to the reduction of cerebral edema, inhibition of astrocyte proliferation, improvement of brain metabolism, and inhibition of neuroinflammation [15–17].

It has been reported in the literature that HBO treatment achieves neuroprotective effects by inhibiting or relieving neuroinflammatory responses, and its mechanism of action may be related to the altered expression of various inflammatory factors such as IL-1β, IL-6, CCL2, IL-10, and TNF-α [13, 18–20]. Consistent with the literature, we found that the expression of several chemokines and their effector receptors are increased after TBI and promote neuroinflammation by regulating neuronal-glial interactions [4, 15, 21]. Through *in vitro* studies, our group found that HBO therapy can downregulate the expression of chemokines CXCL1 and CCL2 and affect inflammatory responses by inhibiting the LPS-induced NF-κB/ MAPKs (JNK and ERK)- CCL2/CXCL1 inflammatory pathway [17]. In the present study, we further examined whether HBO therapy exerts neuroprotective effects by modulating the NF-κB/ MAPKs-CXCL1 inflammatory pathway through *in vivo* studies.

Materials And Methods

Animals and surgery

The rat TBI model was established by the cortical controlled injury (CCI) method described previously [22, 23]. All experimental treatments were in accordance with the Chinese “Guidelines for the Care and Use of Laboratory Animals”. Healthy adult male Sprague-Dawley rats weighing 230-250 g were purchased from the Experimental Animal Center of Nantong University (Nantong, China). All rats were placed in an environment with constant temperature and humidity and could drink and eat freely in a 12 h day and night cycle (the grouping of rats used for each experiment is shown in Table 1). After intraperitoneal anesthesia with 0.4 mL/100 g chloral hydrate, the rat's head was fixed on a stereotaxic device, a hole with a diameter of 6 mm was drilled in the right parietal bone (3.0 mm behind bregma and 3.0 mm centered on the right side of the sagittal suture), the skull was lifted to expose the dura mater, and a pneumatic impact device (TBI 0310, Precision Systems and Instrumentation, USA) was employed to model moderate TBI. The impact parameters of velocity were 4.0 m/s, depth, 3.0 mm, and dwell time, 15 ms. The sham group underwent the same craniotomy, but without impingement.

Assessment of Neurological Injury

Modified neurological severity scores

The modified neurological severity scores (mNSS) method was used to evaluate neurological function [24]. Briefly, the aspects of the test included motor (6 points), sensory (2 points), balance beam test (6 points), lack of reflexes and abnormal activity (4 points). If the animal did not complete the required movements, one point was awarded. The higher the total score obtained by the animal, the more severe the nerve damage.

Morris water maze test

The Morris water maze (MWM) was used to assess cognitive function by observing the mean escape latency and number of platform crossings [25, 26]. The water maze experiments were conducted in a quiet environment with water temperature maintained at 20 ± 1°C. Before modeling, all rats had been acclimatized for 2 consecutive days to exclude the effects of visual and motor dysfunction on the experiment. In the position navigation test, each rat was subjected to 4 trials per day, 120 s of each trial, 30 s of rest, and 5 min of rest between each trial. Each rat was randomly placed in the water from four positions facing the pool wall, and the platform was hidden 2 cm below the water surface. The escape latency of each rat during the trials was recorded and averaged over the four trials as the average escape latency. If an animal failed to find the platform within 120 s, the escape latency was recorded as 120 s. In the spatial exploration test, after the platform was removed, rats were placed in the pool from the quadrant farthest from the original platform and swam freely for 120 s. The number of times rats crossed the platform was recorded.

Drug Treatment

SD male rats were randomly divided into five groups: Sham, TBI, TBI vehicle, TBI low-dose, and TBI high-dose. The CXCR2 antagonist SB225002 was purchased from Tocris (Bristol, UK). The ERK, JNKand NF-κB

inhibitors, PD98059, SP600125, and BAY117082, respectively, were purchased from Calbiochem (Merck, Darmstadt, Germany). The antagonist and the three inhibitors were dissolved in dimethyl sulfoxide (DMSO) and diluted with PBS to a low dose of 2.5 μg/10 μL and a high dose of 25 μg/10 μL, respectively. The TBI +vehicle group was treated with DMSO and PBS. One hour after TBI, different concentrations of antagonist and three different concentrations of inhibitors were injected into the cortex in the center of the injured area using a 10 μL Hamilton microsyringe for approximately 10 min (1 μL/min), after which the needle was left in place for approximately 5 min and then gently and slowly withdrawn [27,28]. The TBI vehicle group was injected in the same way. All rats were injected continuously for 3 days.

HBO Therapy

SD male rats were randomly divided into four groups: sham, sham +HBO, TBI, and TBI +HBO. The rats in the sham +HBO group and TBI +HBO group were subjected to continuous HBO therapy once a day [15]. Rats were placed in a hyperbaric chamber and the pressure in the chamber was slowly increased to 0.2 MPa for about 15 min, then maintained at 0.2 MPa for about 60 min, and finally slowly decreased to atmospheric pressure for 15 min before moving the rats out of the hyperbaric chamber. During treatment, the oxygen concentration in the chamber was kept above 95%.

Immunofluorescent Staining

After rats were anesthetized and rapidly perfused with 4% paraformaldehyde, brain tissues were removed and placed in 4% paraformaldehyde at 4°C overnight for post-fixation. The brain tissues were placed in 20% sucrose for dehydration for 2 days and then replaced with 30% sucrose for dehydration for another 2 days. The brain tissues were cryosectioned to a thickness of 20 μm and further immune-stained with fluorescence. Briefly, sections were incubated with 1% BSA at room temperature, and next incubated overnight at 4°C with the following antibodies: CXCL1 antibody (A00533, rabbit, 1:50, Boster, Wuhan, Hubei, China), CXCR2 antibody (BA0732-2, rabbit, 1:50, Boster, Wuhan, Hubei, China), GFAP antibody (astrocyte marker, MAB360, mouse, 1:1000, Millipore, Billerica, MA, USA), IBA-1 antibody (microglial cell marker, ab5076, goat, 1:500, abcam, Boston, USA) and NeuN antibody (neuron marker, MAB377, mouse , 1:1,000, Millipore, Billerica, MA, USA). The next day, the sections were incubated with Cy3-linked secondary antibody or Alexa 488-linked secondary antibody (1:1000, Jackson ImmunoResearch, West Grove, PA) for 2 h at room temperature. The stained sections were rinsed three times on a shaker for 15 min each, then air dried and sealed on slides. The stained slides were observed by a Nikon fluorescence microscope and images were captured by CCD Spot.

Real-time fluorescence quantitative PCR

Total RNA was extracted from the cerebral cortex of the injured area using Trizol reagent (Invitrogen). Total RNA (1 μg) was reverse transcribed into cDNA according to the manufacturer's instructions (Takara, Shiga, Japan). After addition of SYBR green I, RT-qPCR analysis was performed in a real-time detection system (Rotor-Gene 6000, Hamburg, Germany). The primers used are listed in Table 2. The PCR amplification program was as follows: first pre-denaturation at 95°C for 3 min, followed by 40 thermal

cycles at 95°C for 10 s, 60°C for 30 s, and finally 95°C for 15 s, 60°C for 60 s, and 95°C for 15 s to generate the melting curve. The melting curves were used to ensure that there were no nonspecific products. Quantitative analysis was performed by the $2^{-\Delta\Delta CT}$ method.

Enzyme-Linked Immunosorbent Assay (ELISA)

The rat CXCL1 ELISA kit was purchased from Hangzhou MultiSciences (Lianke) Biotech (EK396/2-96, Hangzhou, Zhejiang, China), and the rat CXCR2 ELISA kit was purchased from Cloud-Clone systems (SEC006Ra, Katy, TX, USA). Protein solution from the damaged area of the cerebral cortex was added to 1.5 mL EP tubes containing 250 μL protein lysate and homogenized. The lysis reaction proceeded for 30 min, and the supernatant was collected by centrifugation. The total protein concentration was measured by BCA protein assay (Pierce, Rockford, IL, USA). The sample volume was 100 μg per well, and ELISA was performed according to the manufacturer's instructions. The absorbance of each well was measured at 450 nm and the target protein concentration was calculated based on a standard curve.

Western Blot Analysis

Protein samples for western blot analysis were prepared in the same way as for ELISA. Protein samples (30 μg) were separated on 10% SDS-PAGE gels and transferred to PVDF membranes. The membranes were blocked with 5% BSA for 2 h at RT to avoid non-specific binding. Following incubation with antibodies, such as p-ERK (9101, rabbit, 1:1000, Cell Signaling, Boston, USA), p-JNK (4688, rabbit, 1:1000, Cell signaling, Boston, USA), p-NF-κB (3033, rabbit, 1:1000, Cell signaling, Boston, USA), or GAPDH antibody (MAB374, mouse, 1:10,000, Millipore, Billerica, MA, USA), at 4°C overnight, the membranes were further incubated with IRDye 800CW antibody for 2 h in the dark at RT. Images were captured using the Odyssey Imaging System (LI-COR Bioscience, Lincoln, NE), and grayscale values were analyzed using Image J software (NIH, Bethesda, MD, USA).

TUNEL Staining

Samples for TUNEL staining were prepared in the same way as described for immunofluorescence double staining. Apoptosis was detected by terminal deoxynucleotidyl transferase-mediated dUTP nick 3’ end labeling (TUNEL) using an apoptosis detection kit (Vazym), according to the manufacturer's instructions. After completion of apoptosis staining, nuclei were stained with DAPI. The stained slides were examined with a Nikon fluorescence microscope and images were obtained with a CCD Spot camera. TUNEL-positive cells in the cerebral cortex of the injured area were counted in each slide using Image J software (NIH, Bethesda, MD, USA).

Statistical Analysis

All data were expressed as MEAN ± SEM. Image J was used to count the number of TUNEL-positive cells and immunofluorescence double-label staining. For western blotting, ImageJ was used to measure the grayscale values of specific bands. The relative expression levels of p-ERK, p-JNK, and p-NF-κB were

standardized to the level of GAPDH. A two-way ANOVA was used to analyze the escape latency and mNSS scores after HBO therapy, and Bonferroni post-test to compare replicate means by row. Multi-group comparisons were performed using one-way ANOVA with post hoc Bonferroni correction. All data were analyzed using GraphPad Prism 5.0 (San Diego, CA, USA).

Results

CXCL1 is predominantly expressed in cerebral cortex astrocytes after TBI

To visualize the cellular localization of CXCL1 in the cortex, we performed immunofluorescence double staining of CXCL1 with the astrocyte marker GFAP, the neuronal marker NeuN, and the microglia marker IBA-1, respectively. As shown in Figure 1, about 69% of CXCL1 was co-labeled with GFAP, about 30% with NeuN, and about 1% with IBA-1. The results suggested that CXCL1 was mainly expressed in astrocytes in the cortex of the injured area after TBI.

Figure 1. CXCL1 is expressed in astrocytes in the cortex of the injured area after TBI. CXCL1 is co-labeled with astrocyte marker GFAP (A-C). Some co-localization is visible with neuronal marker NeuN (D-F), and to a lesser extent the microglial marker IBA-1 (G-I). Co-labeling rate of CXCL1 with astrocytes is about 69%, with neurons 30%, and with microglia about 1% (J) (Bar=20 μm).

CXCR2 is mainly expressed in cerebral cortex neurons after TBI

To confirm the cellular localization of CXCR2 in the cortex, we employed immunofluorescence double staining of CXCR2 with the cellular markers GFAP, NeuN, and IBA-1, respectively. Figure 2 shows that about 85% of CXCR2 was co-labeled with the neuronal marker NeuN, 13% with the microglial marker IBA-1, and 2% with the astrocyte marker GFAP. The results indicated that CXCR2 was mainly expressed in neurons in the cortex of the injured area after TBI.

Figure 2. CXCR2 is expressed in neurons in the cortex of the injured area after TBI. CXCR2 is co-labeled with neuronal marker NeuN (D-F). Minimal co-labeling is visible with astrocyte marker GFAP (A-C) and microglial marker IBA-1 (G-I). Co-labeling rate of CXCR2 with astrocytes is about 2%, with neurons about 85%, and with microglia about 13% (J) (Bar=20 μm).

Upregulated CXCL1 and CXCR2 mRNA and protein expression in rat cerebral cortex after TBI

The expression level of CXCL1 and CXCR2 mRNA and protein were measured by RT-qPCR and ELISA, respectively, in the peri-injured cortex at 1, 3, 7, and 10 days after TBI. As shown in Figure 3A, the mRNA expression levels of CXCL1 and CXCR2 peaked on the first day and then decreased compared with the sham group. The protein expression of inflammation-related factors CXCL1 and CXCR2, as shown in Figure 3B, peaked on the first and third day, respectively, and then showed a decreasing trend compared with the sham group.

Figure 3. mRNA and protein expression of CXCL1 and CXCR2 are upregulated after TBI. (A) Compared to sham, mRNA expression of CXCL1 and CXCR2 after TBI peaks on the first day and then decreases. All values are expressed as mean ± SEM (n 6). (B) Compared to sham, expression of CXCL1 and CXCR2 protein after TBI peaks on the first and third day, respectively, and then decreases. ***p <0.001, *p <0.05.

Up-regulated p-ERK, p-JNK, and p-NF-κB is upregulatedexpression in rat cerebral cortex after TBI

The expression trends of p-ERK, p-JNK, and p-NF-κB in the cortex of the injured area were assessed by western Blot at 1, 3, 7, and 10 days after TBI. As shown in Figure 4, compared with the sham group, p-ERK and p-JNK peaked on the third day after TBI, whereas p-NF-κB showed a decreasing trend after peaking on the first day after TBI.

Figure 4. Up-regulation of p-ERK, p-JNK, and p-NF-κB after TBI. p-ERK and p-JNK expression peaks on the third day after TBI, and p-NF-κB is decreased after peaking on the first day after TBI. Values are expressed as mean ± SEM. ***p < 0.001, **p < 0.01, *p < 0.05, vs. sham.

Increased apoptosis of cortical neurons in the injured area after TBI in rats

TUNEL staining was employed to detect apoptosis at 1, 3, and 7 days after TBI. Figure 5 shows that the number of TUNEL-positive cells increased at 1, 3, and 7 days after TBI compared with the sham group and showed a decreasing trend after reaching a peak on the first day.

Figure 5. Increased apoptosis of neuronal cells in the damaged cortex after TBI. (A-C) TUNEL-positive cells (green), DAPI (blue) and TUNEL+ DAPI merge. (D-G) Apoptosis-positive cells in the injured cortex at 1, 3, and 7 d after TBI. (H) TUNEL-positive cells decrease after peaking on the first day. Values are expressed as mean ± SEM. *** p <0.001, *p <0.05, vs. sham (Bar=20 μm).

CXCR2 antagonist improves neurological function in TBI Rats

To evaluate the effect of CXCL1-CXCR2 on the neurological function of TBI rats, mNSS was scored after cortical injection of CXCR2 antagonist in the injured area of TBI rats. As shown in Figure 6, the mNSS of rats after TBI was significantly higher than that of the sham group with impaired neurological function. The mNSS score of the TBI +high dose group was lower than that of the TBI+vehicle group after successive 3 days local injection of CXCR2 antagonist in the brain injury area, indicating that down-regulation of CXCR2 expression improves neurological function.

Figure 6. Improvement of neurological function in TBI rats after application of high dose of CXCR2 antagonist. mNSS scores decrease in TBI rats after application of high-dose CXCR2 antagonist SB225002. Values are expressed as mean ± SEM. ***p <0.001, vs. TBI vehicle; ###p <0.001, vs. sham.

CXCR2 antagonist improves cognitive function in TBI Rats

To evaluate the effect of CXCL1-CXCR2 on the cognitive function of TBI rats, the number of platform crossings and the average escape latency were observed after cortical injection of CXCR2 antagonist in

the injured area of TBI rats. As shown in Figure 7, compared with the sham group, the escape latency of TBI rats was significantly prolonged and the number of platform crossings was reduced. The escape latency of the TBI +high dose group was lower than that of the TBI + vehicle group, while the number of platform crossings was higher.

Figure 7. Cognitive function of TBI rats is improved after application of high-dose CXCR2 antagonist SB225002. (A) The escape latency in TBI rats is shortened after high dose of CXCR2 antagonist. (B) The number of platform crossings in TBI rats is increased after high dose of CXCR2 antagonist. Values are expressed as mean ± SEM. $^{**}p < 0.01$, $^{*}p < 0.05$, vs. TBI vehicle; $^{###}p < 0.001$, vs. sham.

CXCR2 antagonist inhibits neuronal apoptosis in TBI rats.

To evaluate the effect of CXCR2 antagonist on the apoptosis of cortical neurons in the brain injury area of TBI rats, we performed TUNEL staining. As shown in Figure 8, the number of TUNEL-positive cells in the cerebral cortex of TBI +high dose rats was significantly reduced compared with that in the TBI +vehicle group.

Figure 8. Decreased neuronal apoptosis in TBI rats after application of CXCR2 antagonist SB225002. (A-E) The number of TUNEL-positive cells in the cortex of the injured area 3 days after injury in sham, TBI, TBI vehicle, TBI low dose, and TBI high dose. (F) The number of TUNEL-positive cells in the cortex of TBI rats in the injury area is significantly reduced after application of high dose of CXCR2 antagonist. Values are expressed as mean ± SEM. $^{***}p < 0.001$, vs. TBI vehicle; $^{###}p < 0.001$, vs. sham.

ERK, JNK, and NF-κB inhibitors downregulate mRNA expression of CXCL1, CXCR2 in TBI rats

To verify whether ERK, JNK, and NF-κB regulate the expression of CXCL1/CXCR2, the expression changes of CXCL1/CXCR2 were observed after application of their inhibitors PD98059, SP600125, and BAY117082, respectively. As shown in Figure 9, the mRNA expression of CXCL1 and CXCR2 decreased significantly after 3 days of continuous injection of high doses of ERK, JNK, and NF-κB inhibitors compared with the TBI +vehicle group, indicating that ERK, JNK, and NF-κB could regulate CXCL1 and CXCR2.

Figure 9. ERK, JNK, and NF-κB inhibitors PD98059, SP600125, and BAY117082 down-regulate CXCL1 and CXCR2 mRNA expression. (A) CXCL1 mRNA expression is decreased 3 days after continuous injection of high doses of ERK, JNK, and NF-κB inhibitors. (B) CXCR2 mRNA expression is decreased 3 days after continuous injection of high doses of ERK, JNK, and NF-κB inhibitors. Values are expressed as mean ± SEM. $^{***}p < 0.001$, $^{**}p < 0.01$, $^{*}p < 0.05$, vs. TBI vehicle; $^{###}p < 0.001$, $^{##}p < 0.01$, vs. sham.

HBO improves neurological function in TBI rats

The effect of HBO therapy on the neurological function of TBI was observed by mNSS score. We found that after HBO treatment, the mNSS score of the TBI +HBO group was significantly lower than that of the

TBI group at 3, 7, and 10 days after TBI, and HBO therapy could improve the neurological function of rats after TBI , shown in Figure 10.

Figure 10. HBO therapy improves neurological function in TBI rats. mNSS scores are lower in after TBI+HBO than TBI alone at 3, 7, and 10 days after TBI. Values are expressed as mean ± SEM. $^{**}p < 0.01$, $^{*}p < 0.05$.

HBO treatment improved the cognitive function of rats after TBI

The Morris water maze was used to assess the effect of HBO on cognitive function in rats. In the locomotor navigation test, as shown in Figure 11A, the escape latency was significantly shorter in the TBI + HBO group than in the TBI group on days 5 and 6. In the 7-day spatial exploration trial after TBI, the number of platforms traversed by the TBI +HBO group was significantly higher than that of the TBI group. From these results, we can see that HBO treatment can improve the cognitive function of rats after TBI.

Figure 11. HBO treatment improves cognitive function in TBI rats. (A) In the locomotor navigation test, the escape latency is significantly lower after TBI+HBO than in TBI on days 5 and 6. (B) In the exploration test, the number of platform crossings is higher after TBI+HBO than TBI alone. Values are expressed as mean ± SEM. $^{***}p < 0.001$, $^{*}p < 0.05$.

HBO treatment inhibits neuronal apoptosis in rats with TBI

We evaluated the effect of HBO treatment on neuronal cell apoptosis in the cerebral cortex of rats with TBI. In Figure 12, the results show that the number of TUNEL-positive cells in the cerebral cortex of the TBI +HBO group was significantly reduced compared with the TBI group, indicating that HBO treatment could inhibit apoptosis of neuronal cells in TBI rats.

Figure 12. Decreased neuronal apoptosis in TBI rats after HBO treatment. (A-D) The number of TUNEL-positive cells (Bar=20 μm) in the cortex of the injured area 3 days after injury in sham, sham+HBO, TBI and TBI+HBO. (E) The number of TUNEL-positive cells in the cortex of TBI rats in the injury area after HBO treatment is significantly reduced compared to TBI alone. Values are expressed as mean ± SEM. $^{*}p < 0.05$.

HBO treatment downregulates CXCL1 and CXCR2 mRNA and protein expression after TBI in rats

To verify whether HBO treatment regulates expression of CXCL1/CXCR2, the mRNA and protein contents of CXCL1 and CXCR2 were detected by RT-qPCR and ELISA, respectively, after 3 days of continuous HBO therapy. In Figure 13, the results show that the mRNA and protein expression of CXCL1 and CXCR2 were significantly decreased compared with the TBI group, indicating that HBO treatment could down-regulate the expression of CXCL1 and CXCR2.

Figure 13. HBO treatment down-regulates mRNA and protein expression of CXCL1, CXCR2. (A) mRNA expression of CXCL1 and CXCR2 decreases after 3 days of HBO treatment. (B) protein expression of

CXCL1 and CXCR2 decreases after 3 days of HBO treatment. Values are expressed as mean ± SEM. ***$p < 0.001$, *$p < 0.05$.

HBO treatment down-regulates the expression of p-ERK, p-JNK, and p-NF-κB after TBI in rats

To verify whether HBO therapy regulates CXCL1/CXCR2 expression by modifying ERK, JNK, and NF-κB, we tested the expression level of p-ERK, p-JNK, and p-NF-κB proteins by western blot after 3 days of continuous HBO treatment. In Figure 14, the results show that the levels of p-ERK, p-JNK, and p-NF-κB were significantly lower in the TBI +HBO group compared with the TBI group, suggesting that HBO treatment inhibits expression of CXCL1 and CXCR2 by downregulating the expression of p-ERK, p-JNK, and p-NF-κB.

Figure 14. HBO treatment down-regulates expression of ERK, JNK, and NF-κB. p-ERK, p-JNK, and p-NF-κB expression is significantly decreased after continuous HBO treatment for 3 days compared to TBI alone. Values are expressed as mean ± SEM. **$p < 0.01$; *$p < 0.05$.

Discussion

Neuroinflammation is an important early reversible process underlying secondary injury following TBI, and thus a promising therapeutic target. Activation and proliferation of glial cells (astrocytes and microglia) in damaged brain can harm nerve cells by releasing cytokines and chemokines [29]. Chemokines are divided into pro-inflammatory and anti-inflammatory factors, and after the occurrence of TBI, chemokines help attract a wide range of immune cells to the site of injury [30]. Numerous such inflammatory mediators have been detected in both TBI animal models and patients, including CCL2, CCL3, CXCL1, CXCL2, CXCL10, CXCL12, CCR2, CCR5, CXCR4, and CX3CR1 [9, 21, 31–35]. These chemokines act as chemoattractants for peripheral blood leukocytes that can produce further damage through direct cellular toxicity. In TBI, CCL2/CCR2 is involved in disease progression, and CCL2 is one of the chemokines that is significantly upregulated within 24 h of injury in TBI animal models [4]. CCL2 has also been detected in cerebrospinal fluid, serum, and brain tissue from TBI patients, and animal studies showed that down-regulation of CCR2 expression significantly improved neurological function in TBI rats [36–39]. CXCL12/CXCR4 signaling is also involved in the pathological progression of TBI [35, 40]. On days 3 and 7 after TBI, upregulation of CXCR4 expression has been observed in the cortex surrounding the injured area, and intracranial injection of CXCL12 induced angiogenesis, improved edema, reduced blood brain barrier permeability, and decreased the number of apoptotic cells [41].

The cytokine CXCL1 contributes to neuroinflammation primarily through binding to CXCR2 [42, 43]. In TBI model rats, local expression of CXCL1 peaked within 4 h after injury and was sustained for hours thereafter [4]. Joanna and colleagues reported that choroidal epithelial cells induced neutrophil infiltration after TBI by secreting CXC-family chemokines [44]. In this study, we found that the number of apoptotic cells increased in the cortical vicinity of the injured area after TBI, and neurological function was impaired. The expression of CXCL1 and CXCR2 increased after TBI, and cell localization experiments revealed that CXCL1 was mainly expressed in astrocytes, while CXCR2 was expressed in neurons. The

decrease in neuronal apoptosis and improvement in neurological function after application of an CXCR2 antagonist suggested that CXCL1-CXCR2 mediated the interaction between activated astrocytes and neurons after TBI, aggravating secondary injury. Collectively, these results suggest that CXCL1 signaling induces a sustained intracerebral inflammatory response in the hours and days following TBI. Our previous studies showed that during inflammation, CXCL1 expression in primary cultured astrocytes increased through the NF-κB, ERK, and JNK signaling pathways, and that CXCL1 binding to its receptor mediated the inflammatory response, thereby playing an important role in TBI[17]. We further found that the expression of p-ERK, p-JNK, and p-NF-κB increased after TBI, while ERK, JNK, and NF-κB inhibitors decreased the expression of CXCL1 and CXCR2, suggesting that ERK, JNK and NF-κB can exert neuroinflammatory effects by regulating downstream CXCL1 after TBI in rats. Thus, the NF-κB/ MAPKs (JNK and ERK)- CXCL1 inflammatory pathway has a role in post-TBI neuroinflammation.

HBO treatment exerts neuroprotective effects by modulating multiple neuroinflammatory pathways after neurological injury. After spinal cord injury in rats, HBO treatment inhibits the high-mobility group protein B1/ NF-κB and Toll-like receptor 2 signaling pathways, thus reducing secondary injury caused by inflammation and promoting the recovery of neurological function [45, 46]. Some animal studies have shown that HBO treatment reduced the expression of caspase-3, TNF-α, IL-6, and IL-1β by inhibiting the Toll-like receptor 4/NF-κB signaling pathway after TBI in rats, thus reducing the secondary injury caused by inflammation after TBI and promoting the recovery of neurological function [20]. IL-10 plays an important role in the neuroprotective effects of HBO on TBI, and IL-10 deficiency leads to increased brain damage after TBI and decreased suppression of neuroinflammation by HBO [18]. HBO therapy can reduce neuronal apoptosis in the acute phase of TBI by regulating the Akt/GSK3β/β-catenin pathway [12]. We showed in a previous study that HBO therapy modulates the NF-κB/MAPKs -CXCL1 signaling pathways to suppress inflammation induced by lipopolysaccharide in primary astrocytes of neonatal rats [17]. In the present study, we found that HBO therapy could downregulate the expression of p-ERK, p-JNK, p-NF-κB, CXCL1 and CXCR2, while reducing neuronal apoptosis and improving the motor, sensory, and cognitive neurological functions of TBI rats, ultimately alleviating secondary injury. In summary, the results of this study suggest that HBO therapy can play a neuroprotective role by regulating the NF-κB/ MAPKs (JNK, and ERK)- CXCL1 inflammatory pathway to modulate neuroinflammation.

Conclusion

Post-TBI CXCL1-CXCR2 mediates the interaction of activated astrocytes and neurons, exacerbating secondary injury. HBO therapy can exert neuroprotective effects by regulating the NF-κB/ MAPKs (JNK, and ERK)- CXCL1 inflammatory pathway to modulate neuroinflammation after TBI. This study provides theoretical and experimental evidence for the clinical use of HBO in the treatment of brain injury.

Abbreviations

TBI: traumatic brain injury; CCI: controlled cortical impact; HBO: hyperbaric oxygen; CXCL1: Chemokine (C-X-C motif) ligand 1; CXCR2: chemokine C-C motif receptor 2; CCL2: chemokine C-C motif ligand 2; CCR2:

Chemokine C-C motif receptor 2; MAPKs: mitogen-activated protein kinases; NF-κB: nuclear factor-kappa B; JNK: c-Jun N-terminal kinase; ERK: extracellular signal-regulated kinase; GFAP: glial fibrillary acidic protein; IBA-1: ionized calcium binding adapter molecule 1; NeuN: neuronal nuclei; TUNEL: terminal deoxynucleotidyl transferase-mediated dUTP nick-end labeling; DAPI: 6-diamidino-2-phenylindole; DMSO: Dimethyl sulfoxide; ELISA: enzyme-linked immunosorbent assay; RT-qPCR: real-time quantitative PCR

Declarations

Ethics approval and consent to participate

The protocol of this study was approved by the Experimental Animal Center of Nantong University (permission number: 20191106-003).

Consent for publication

Not applicable.

Availability of data and materials

All data used during the current study available from the corresponding author on reasonable request.

Conflict of Interest

The authors declare that they have no conflicts of interest related to this study.

Funding

This project was funded by the National Natural Science Foundation of China (No. 81702223), and the Science and Technology Planning Project of Nantong (MS22019006).

Authors' contributions

Anqi Xia, Huan Huang, Wenjun You, Ying Liu, Hongqin Wu, Su Liu performed the experiments. Su Liu conceived and designed the study. Ying Liu and Hongqin Wu analyzed the data. All authors read and approved the final manuscript.

Acknowledgements

We thank the staff members of our team for their cooperation in this work.

References

1. Khellaf A, Khan DZ, Helmy A. Recent advances in traumatic brain injury. J Neurol. 2019;266:2878-89.
2. Jiang JY, Gao GY, Feng JF, Mao Q, Chen LG, Yang XF, et al. Traumatic brain injury in China. Lancet Neurol. 2019;18:286-95.

3. Kumar A, Stoica BA, Loane DJ, Yang M, Abulwerdi G, Khan N, et al. Microglial-derived microparticles mediate neuroinflammation after traumatic brain injury. J Neuroinflammation. 2017;14:47.
4. Dalgard CL, Cole JT, Kean WS, Lucky JJ, Sukumar G, McMullen DC, et al. The cytokine temporal profile in rat cortex after controlled cortical impact. Front Mol Neurosci. 2012;5:6.
5. Di Battista AP, Rhind SG, Hutchison MG, Hassan S, Shiu MY, Inaba K, et al. Inflammatory cytokine and chemokine profiles are associated with patient outcome and the hyperadrenergic state following acute brain injury. J Neuroinflammation. 2016;13:40.
6. Deng Y, Jiang X, Deng X, Chen H, Xu J, Zhang Z, et al. Pioglitazone ameliorates neuronal damage after traumatic brain injury via the PPARgamma/NF-kappaB/IL-6 signaling pathway. Genes Dis. 2020;7:253-65.
7. Finnie JW. Neuroinflammation: beneficial and detrimental effects after traumatic brain injury. Inflammopharmacology. 2013;21:309-20.
8. Chen Y, Meng J, Bi F, Li H, Chang C, Ji C, et al. EK7 Regulates NLRP3 Inflammasome Activation and Neuroinflammation Post-traumatic Brain Injury. Front Mol Neurosci. 2019;12:202.
9. Morganti-Kossmann MC, Semple BD, Hellewell SC, Bye N, Ziebell JM. The complexity of neuroinflammation consequent to traumatic brain injury: from research evidence to potential treatments. Acta Neuropathol. 2019;137:731-55.
10. Hu Q, Manaenko A, Xu T, Guo Z, Tang J, Zhang JH. Hyperbaric oxygen therapy for traumatic brain injury: bench-to-bedside. Med Gas Res. 2016;6:102-10.
11. Wolf EG, Prye J, Michaelson R, Brower G, Profenna L, Boneta O. Hyperbaric side effects in a traumatic brain injury randomized clinical trial. Undersea Hyperb Med. 2012;39:1075-82.
12. He H, Li X, He Y. Hyperbaric oxygen therapy attenuates neuronal apoptosis induced by traumatic brain injury via Akt/GSK3beta/beta-catenin pathway. Neuropsychiatr Dis Treat. 2019;15:369-74.
13. Wee HY, Lim SW, Chio CC, Niu KC, Wang CC, Kuo JR. Hyperbaric oxygen effects on neuronal apoptosis associations in a traumatic brain injury rat model. J Surg Res. 2015;197:382-9.
14. Daly S, Thorpe M, Rockswold S, Hubbard M, Bergman T, Samadani U, et al. Hyperbaric Oxygen Therapy in the Treatment of Acute Severe Traumatic Brain Injury: A Systematic Review. J Neurotrauma. 2018;35:623-9.
15. Liu S, Shen G, Deng S, Wang X, Wu Q, Guo A. Hyperbaric oxygen therapy improves cognitive functioning after brain injury. Neural Regen Res. 2013;8:3334-43.
16. Liu S, Liu Y, Deng S, Guo A, Wang X, Shen G. Beneficial effects of hyperbaric oxygen on edema in rat hippocampus following traumatic brain injury. Exp Brain Res. 2015;233:3359-65.
17. Liu S, Lu C, Liu Y, Zhou X, Sun L, Gu Q, et al. Hyperbaric Oxygen Alleviates the Inflammatory Response Induced by LPS Through Inhibition of NF-kappaB/MAPKs-CCL2/CXCL1 Signaling Pathway in Cultured Astrocytes. Inflammation. 2018;41:2003-11.
18. Chen X, Duan XS, Xu LJ, Zhao JJ, She ZF, Chen WW, et al. Interleukin-10 mediates the neuroprotection of hyperbaric oxygen therapy against traumatic brain injury in mice. Neuroscience.

2014;266:235-43.

19. Zhang Y, Yang Y, Tang H, Sun W, Xiong X, Smerin D, et al. Hyperbaric oxygen therapy ameliorates local brain metabolism, brain edema and inflammatory response in a blast-induced traumatic brain injury model in rabbits. Neurochem Res. 2014;39:950-60.
20. Meng XE, Zhang Y, Li N, Fan DF, Yang C, Li H, et al. Hyperbaric Oxygen Alleviates Secondary Brain Injury After Trauma Through Inhibition of TLR4/NF-kappaB Signaling Pathway. Med Sci Monit. 2016;22:284-8.
21. Jassam YN, Izzy S, Whalen M, McGavern DB, El Khoury J. Neuroimmunology of Traumatic Brain Injury: Time for a Paradigm Shift. Neuron. 2017;95:1246-65.
22. Beretta S, Cunningham KM, Haus DL, Gold EM, Perez H, Lopez-Velazquez L, et al. Effects of Human ES-Derived Neural Stem Cell Transplantation and Kindling in a Rat Model of Traumatic Brain Injury. Cell Transplant. 2017;26:1247-61.
23. Patel NA, Moss LD, Lee JY, Tajiri N, Acosta S, Hudson C, et al. Long noncoding RNA MALAT1 in exosomes drives regenerative function and modulates inflammation-linked networks following traumatic brain injury. J Neuroinflammation. 2018;15:204.
24. Khatri P, Kleindorfer DO, Devlin T, Sawyer RN, Jr., Starr M, Mejilla J, et al. Effect of Alteplase vs Aspirin on Functional Outcome for Patients With Acute Ischemic Stroke and Minor Nondisabling Neurologic Deficits: The PRISMS Randomized Clinical Trial. JAMA. 2018;320:156-66.
25. Vorhees CV, Williams MT. Morris water maze: procedures for assessing spatial and related forms of learning and memory. Nat Protoc. 2006;1:848-58.
26. Zuo Y, Hu X, Yang Q, Zhao L, Chen X, Lin J, et al. Preoperative vitamin-rich carbohydrate loading alleviates postoperative cognitive dysfunction in aged rats. Behav Brain Res. 2019;373:112107.
27. Gao YY, Zhang ZH, Zhuang Z, Lu Y, Wu LY, Ye ZN, et al. Recombinant milk fat globule-EGF factor-8 reduces apoptosis via integrin beta3/FAK/PI3K/AKT signaling pathway in rats after traumatic brain injury. Cell Death Dis. 2018;9:845.
28. Lin CC, Lee IT, Chi PL, Hsieh HL, Cheng SE, Hsiao LD, et al. C-Src/Jak2/PDGFR/PKCdelta-dependent MMP-9 induction is required for thrombin-stimulated rat brain astrocytes migration. Mol Neurobiol. 2014;49:658-72.
29. Burda JE, Bernstein AM, Sofroniew MV. Astrocyte roles in traumatic brain injury. Exp Neurol. 2016;275 Pt 3:305-15.
30. Helmy A, Antoniades CA, Guilfoyle MR, Carpenter KL, Hutchinson PJ. Principal component analysis of the cytokine and chemokine response to human traumatic brain injury. PLoS One. 2012;7:e39677.
31. Thelin EP, Tajsic T, Zeiler FA, Menon DK, Hutchinson PJA, Carpenter KLH, et al. Monitoring the Neuroinflammatory Response Following Acute Brain Injury. Front Neurol. 2017;8:351.
32. Perez-Polo JR, Rea HC, Johnson KM, Parsley MA, Unabia GC, Xu G, et al. Inflammatory consequences in a rodent model of mild traumatic brain injury. J Neurotrauma. 2013;30:727-40.

33. Dyhrfort P, Shen Q, Clausen F, Thulin M, Enblad P, Kamali-Moghaddam M, et al. Monitoring of Protein Biomarkers of Inflammation in Human Traumatic Brain Injury Using Microdialysis and Proximity Extension Assay Technology in Neurointensive Care. J Neurotrauma. 2019;36:2872-85.
34. Gyoneva S, Ransohoff RM. Inflammatory reaction after traumatic brain injury: therapeutic potential of targeting cell-cell communication by chemokines. Trends Pharmacol Sci. 2015;36:471-80.
35. Chen TJ, Wu WQ, Ying GR, Fu QY, Xiong K. Serum CXCL12 concentration in patients with severe traumatic brain injury are associated with mortality. Clin Chim Acta. 2016;454:6-9.
36. Liu S, Zhang L, Wu Q, Wu Q, Wang T. Chemokine CCL2 induces apoptosis in cortex following traumatic brain injury. J Mol Neurosci. 2013;51:1021-9.
37. Liu R, Liao XY, Tang JC, Pan MX, Chen SF, Lu PX, et al. BpV(pic) confers neuroprotection by inhibiting M1 microglial polarization and MCP-1 expression in rat traumatic brain injury. Mol Immunol. 2019;112:30-9.
38. Semple BD, Frugier T, Morganti-Kossmann MC. CCL2 modulates cytokine production in cultured mouse astrocytes. J Neuroinflammation. 2010;7:67.
39. Woodcock TM, Frugier T, Nguyen TT, Semple BD, Bye N, Massara M, et al. The scavenging chemokine receptor ACKR2 has a significant impact on acute mortality rate and early lesion development after traumatic brain injury. PLoS One. 2017;12:e0188305.
40. Yu P, Zhang Z, Li S, Wen X, Quan W, Tian Q, et al. Progesterone modulates endothelial progenitor cell (EPC) viability through the CXCL12/CXCR4/PI3K/Akt signalling pathway. Cell Prolif. 2016;49:48-57.
41. Sun W, Liu J, Huan Y, Zhang C. Intracranial injection of recombinant stromal-derived factor-1 alpha (SDF-1alpha) attenuates traumatic brain injury in rats. Inflamm Res. 2014;63:287-97.
42. Wu F, Zhao Y, Jiao T, Shi D, Zhu X, Zhang M, et al. CXCR2 is essential for cerebral endothelial activation and leukocyte recruitment during neuroinflammation. J Neuroinflammation. 2015;12:98.
43. Valles A, Grijpink-Ongering L, de Bree FM, Tuinstra T, Ronken E. Differential regulation of the CXCR2 chemokine network in rat brain trauma: implications for neuroimmune interactions and neuronal survival. Neurobiol Dis. 2006;22:312-22.
44. Szmydynger-Chodobska J, Strazielle N, Zink BJ, Ghersi-Egea JF, Chodobski A. The role of the choroid plexus in neutrophil invasion after traumatic brain injury. J Cereb Blood Flow Metab. 2009;29:1503-16.
45. Yang J, Liu X, Zhou Y, Wang G, Gao C, Su Q. Hyperbaric oxygen alleviates experimental (spinal cord) injury by downregulating HMGB1/NF-kappaB expression. Spine (Phila Pa 1976). 2013;38:E1641-8.
46. Tan J, Zhang F, Liang F, Wang Y, Li Z, Yang J, et al. Protective effects of hyperbaric oxygen treatment against spinal cord injury in rats via toll-like receptor 2/nuclear factor-kappaB signaling. Int J Clin Exp Pathol. 2014;7:1911-

Tables

Table1 Number of animals per experiment

	Time			
	1day	3day	7day	10day
Experiment 1				
CXCL1 immunofluorescence		3		
Experiment 2				
CXCR2 immunofluorescence		3		
Experiment 3				
sham qPCR		6		
TBI qPCR	6	6	6	6
sham ELISA		5		
TBI ELISA	5	5	5	5
Experiment 4				
Sham western blot		3		
TBI western blot	3	3	3	3
Experiment 5				
sham+TUNEL		3		
TBI+TUNEL	3	3	3	
Experiment 6				
sham mNSS/MWM/TUNEL		8		
TBI mNSS/MWM/TUNEL		8		
vehicle mNSS/MWM/TUNEL		8		
SB225002 high dose mNSS/MWM/TUNEL		8		
SB225002 low dose mNSS/MWM/TUNEL		8		
Experiment 7				
sham qPCR		6		
TBI qPCR		6		
vehicle qPCR		6		
PD98059 high dose qPCR		6		
PD98059 low dose qPCR		6		

SP600125 high dose qPCR	6	
SP600125 low dose qPCR	6	
BAY117082 high dose qPCR	6	
BAY117083 low dose qPCR	6	
Experiment 8		
sham mNSS/MWM		8
sham+HBO mNSS/MWM		8
TBI mNSS/MWM		8
TBI+HBO mNSS/MWM		8
Experiment 9		
sham TUNEL	3	
sham+HBO TUNEL	3	
TBI TUNEL	3	
TBI+HBO TUNEL	3	
Experiment 10		
sham qPCR	6	
sham+HBO qPCR	6	
TBI qPCR	6	
TBI+HBO qPCR	6	
sham ELISA	5	
sham+HBO ELISA	5	
TBI ELISA	5	
TBI+HBO ELISA	5	
Experiment 11		
sham western blot	3	
sham+HBO western blot	3	
TBI western blot	3	
TBI+HBO western blot	3	

Table 2. Primer sequences

Genes	Primers	Sequences
GAPDH	Forward	5'-TCCTACCCCCAATGTATCCG-3'
	Reverse	5'-CCTTTAGTGGGCCCTCGG-3'
CXCL1	Forward	5'- GCACCCAAACCGAAGTCATA-3'
	Reverse	5'-GGGGACACCCTTTAGCATCT-3'
CXCR2	Forward	5'- TGGTCCTCGTCTTCCTGCTCTG-3'
	Reverse	5'- CGTTCTGGCGTTCACAGGTCTC-3'

Figures

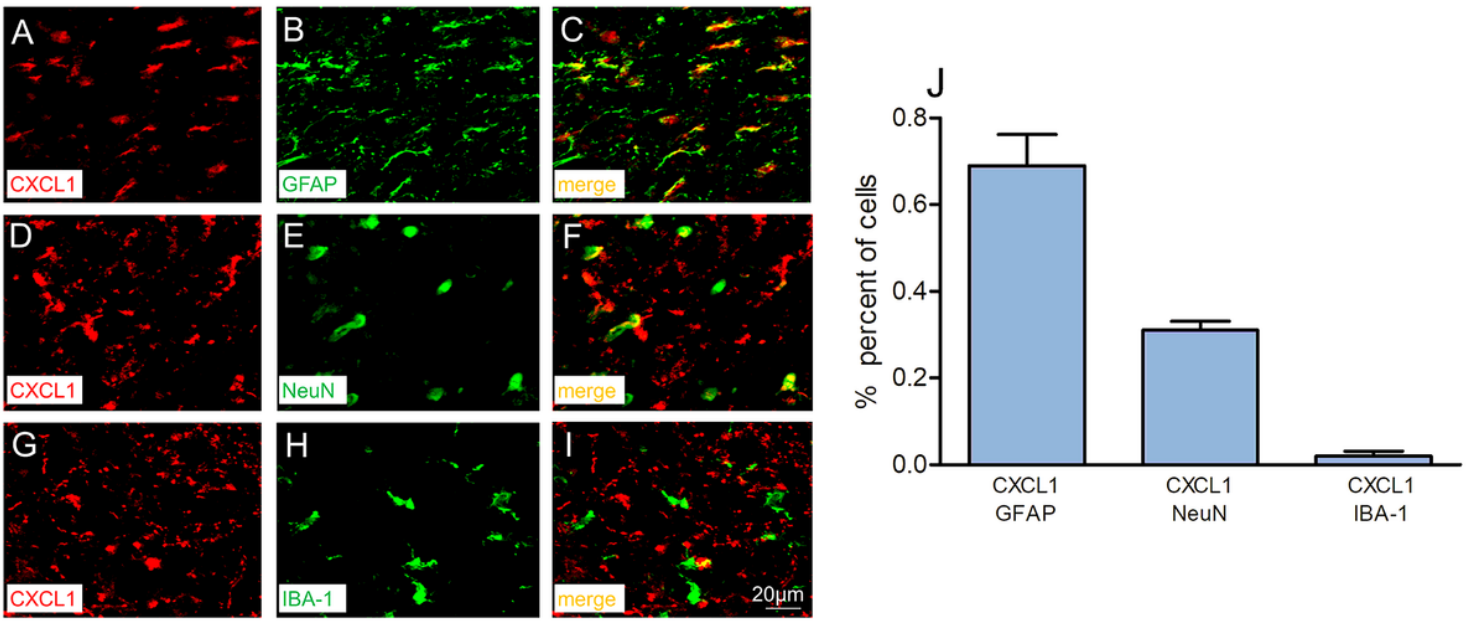

Figure 1

CXCL1 is expressed in astrocytes in the cortex of the injured area after TBI. CXCL1 is co-labeled with astrocyte marker GFAP (A-C). Some co-localization is visible with neuronal marker NeuN (D-F), and to a lesser extent the microglial marker IBA-1 (G-I). Co-labeling rate of CXCL1 with astrocytes is about 69%, with neurons 30%, and with microglia about 1% (J) (Bar=20 μm).

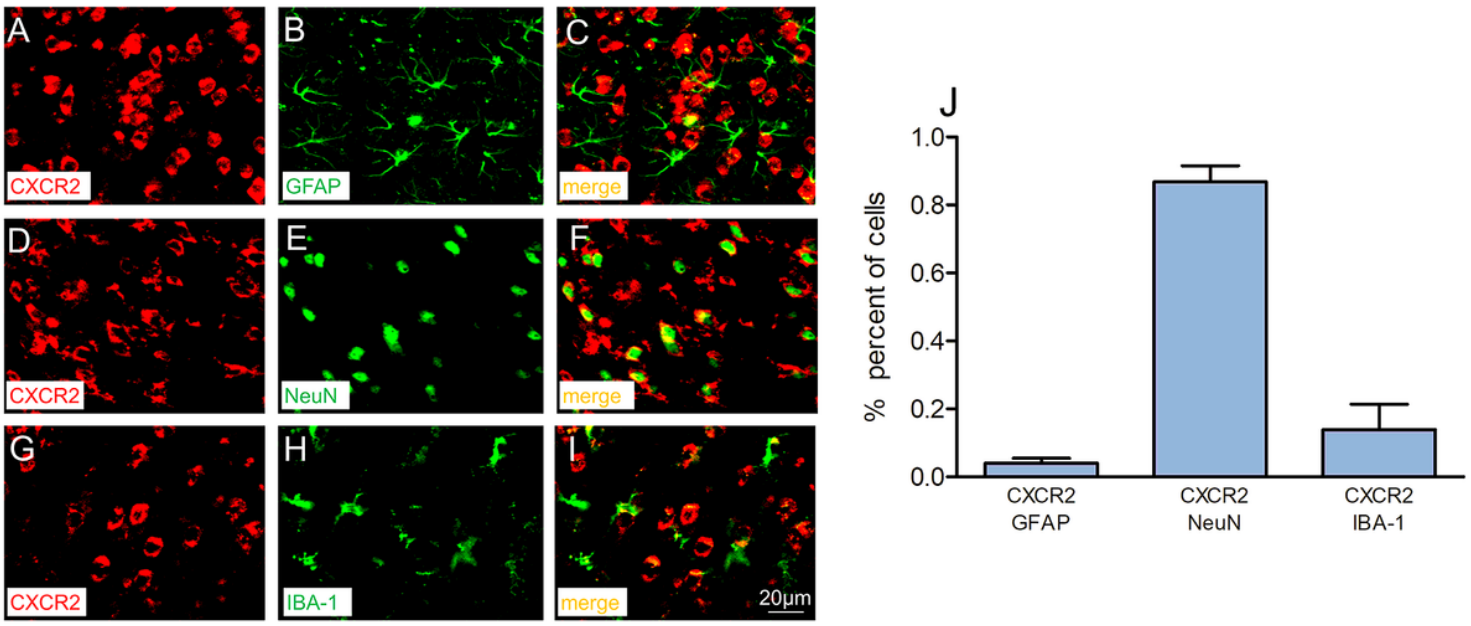

Figure 2

CXCR2 is expressed in neurons in the cortex of the injured area after TBI. CXCR2 is co-labeled with neuronal marker NeuN (D-F). Minimal co-labeling is visible with astrocyte marker GFAP (A-C) and microglial marker IBA-1 (G-I). Co-labeling rate of CXCR2 with astrocytes is about 2%, with neurons about 85%, and with microglia about 13% (J) (Bar=20 μm).

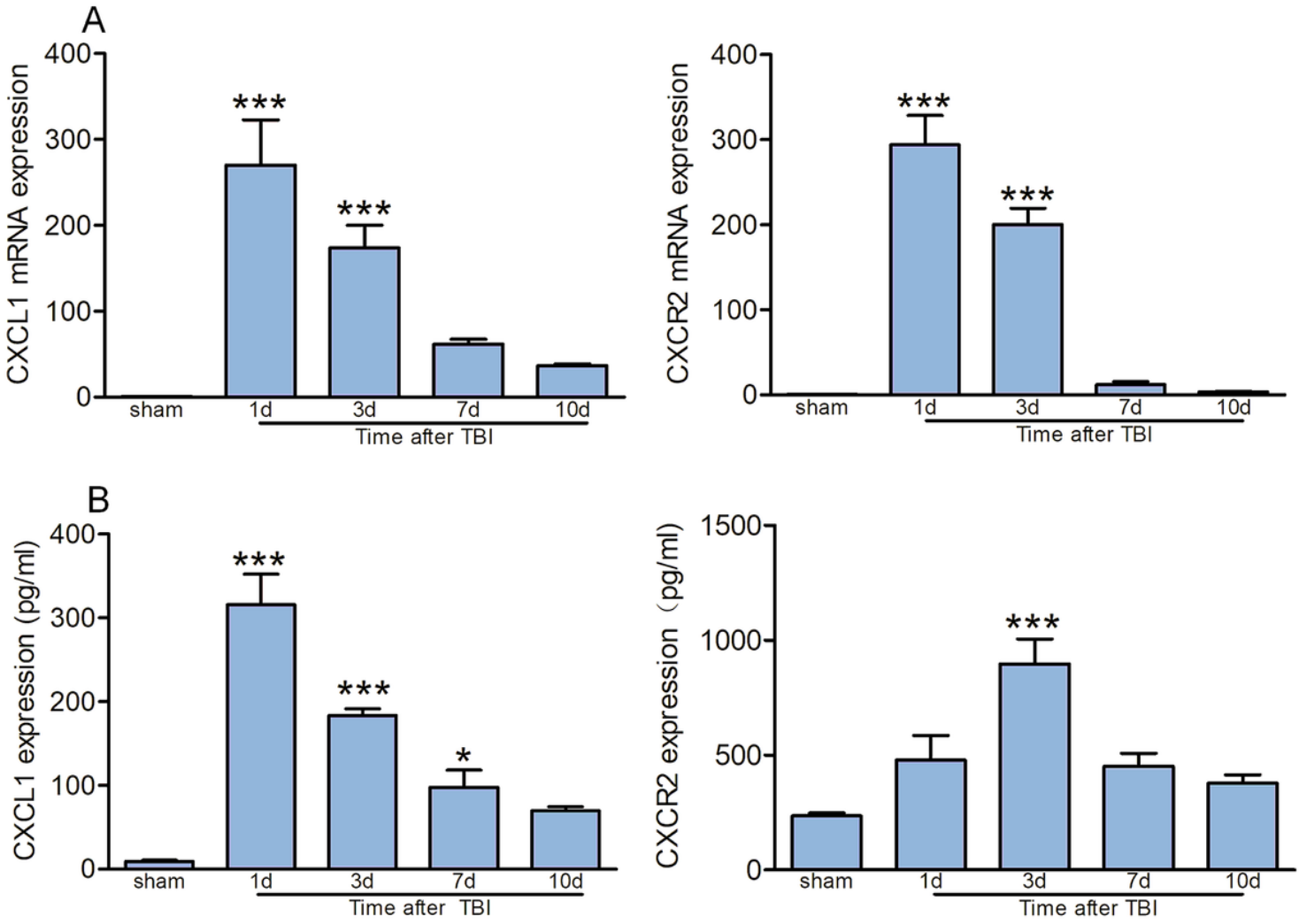

Figure 3

mRNA and protein expression of CXCL1 and CXCR2 are upregulated after TBI. (A) Compared to sham, mRNA expression of CXCL1 and CXCR2 after TBI peaks on the first day and then decreases. All values are expressed as mean ± SEM (n 6). (B) Compared to sham, expression of CXCL1 and CXCR2 protein after TBI peaks on the first and third day, respectively, and then decreases. ***p <0.001, *p <0.05.

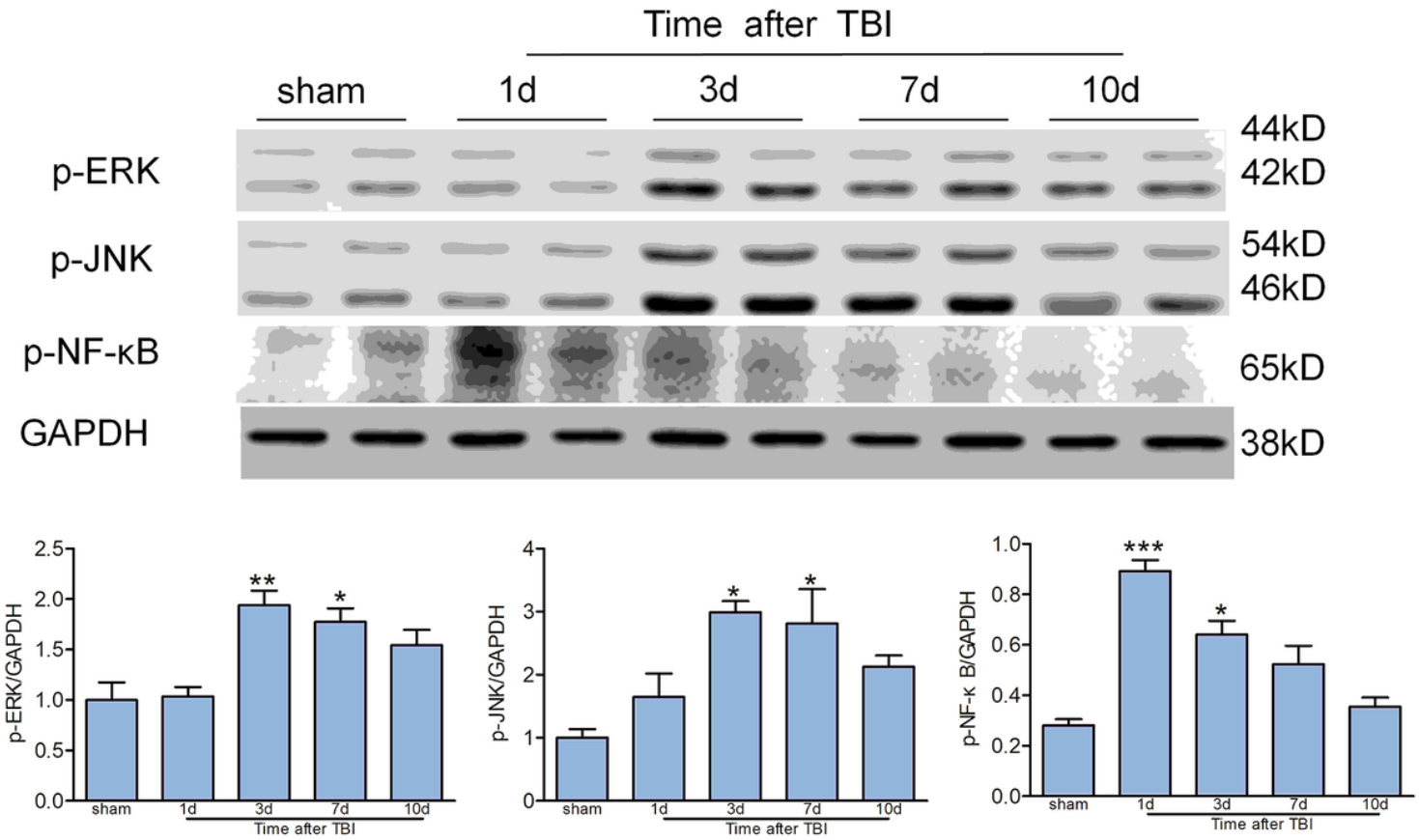

Figure 4

Up-regulation of p-ERK, p-JNK, and p-NF-κB after TBI. p-ERK and p-JNK expression peaks on the third day after TBI, and p-NF-κB is decreased after peaking on the first day after TBI. Values are expressed as mean ± SEM. ***p < 0.001, **p < 0.01, *p < 0.05, vs. sham.

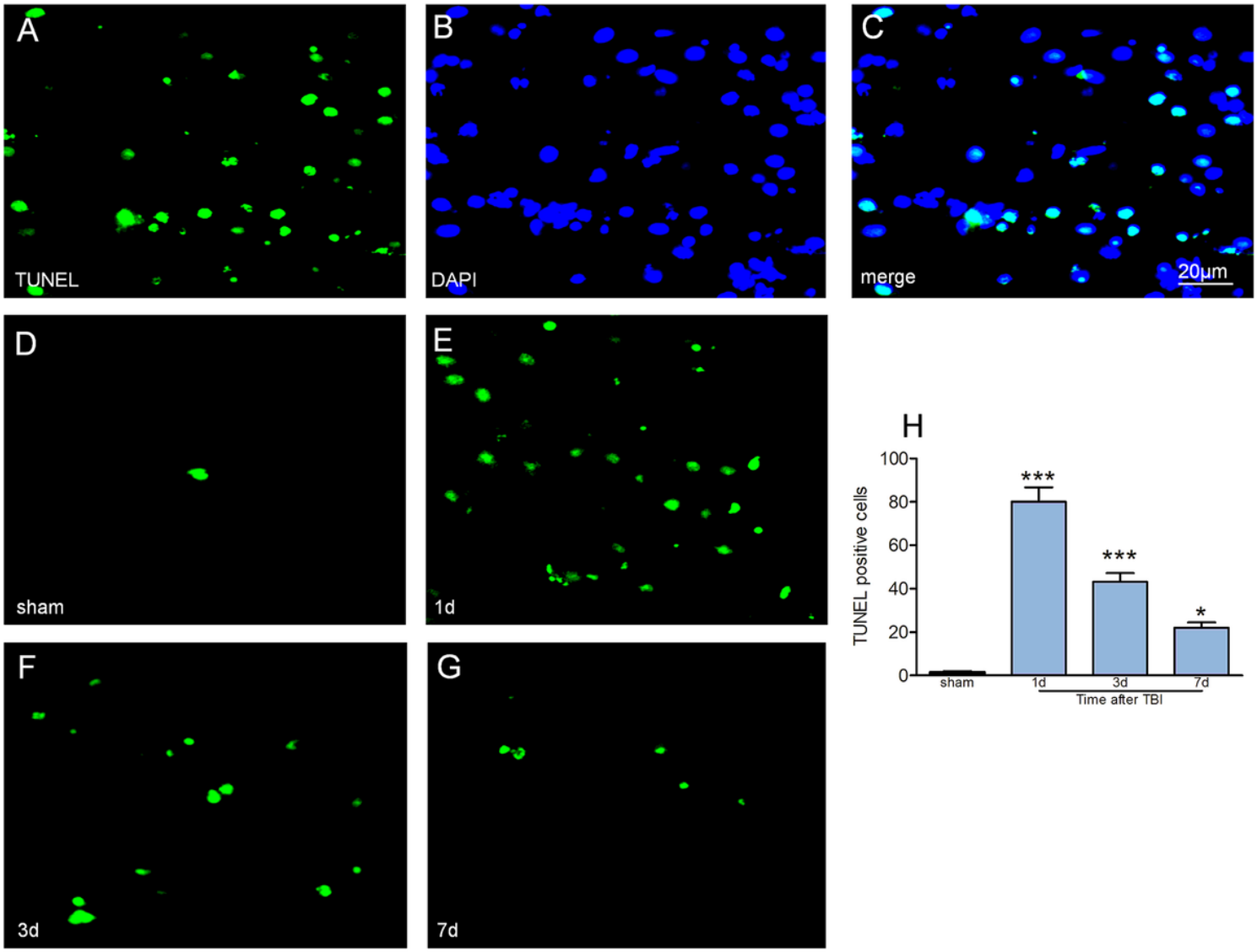

Figure 5

Increased apoptosis of neuronal cells in the damaged cortex after TBI. (A-C) TUNEL-positive cells (green), DAPI (blue) and TUNEL+ DAPI merge. (D-G) Apoptosis-positive cells in the injured cortex at 1, 3, and 7 d after TBI. (H) TUNEL-positive cells decrease after peaking on the first day. Values are expressed as mean ± SEM. *** p <0.001, *p <0.05, vs. sham (Bar=20 μm).

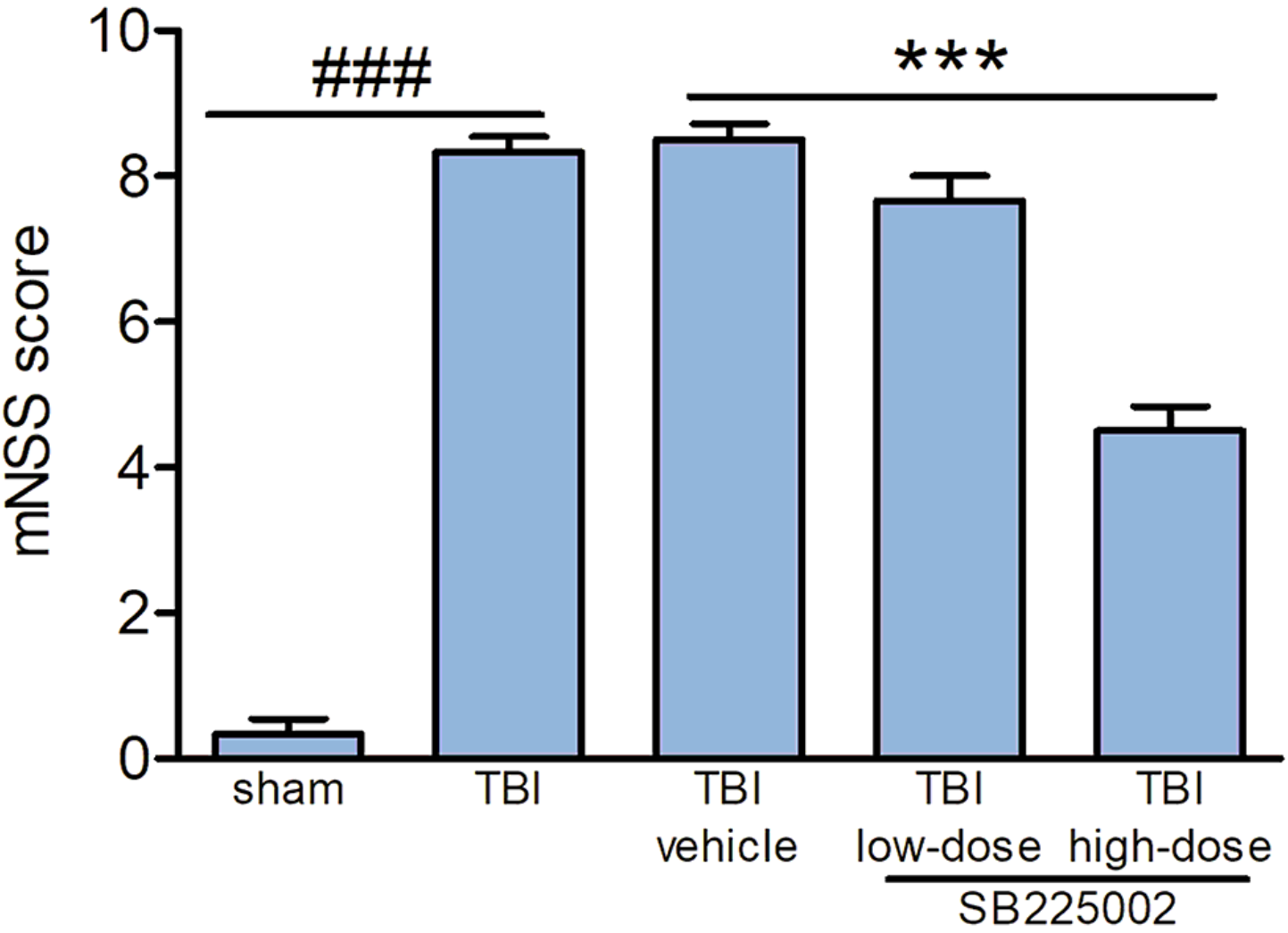

Figure 6

Improvement of neurological function in TBI rats after application of high dose of CXCR2 antagonist. mNSS scores decrease in TBI rats after application of high-dose CXCR2 antagonist SB225002. Values are expressed as mean ± SEM. ***p <0.001, vs. TBI vehicle; ###p <0.001, vs. sham.

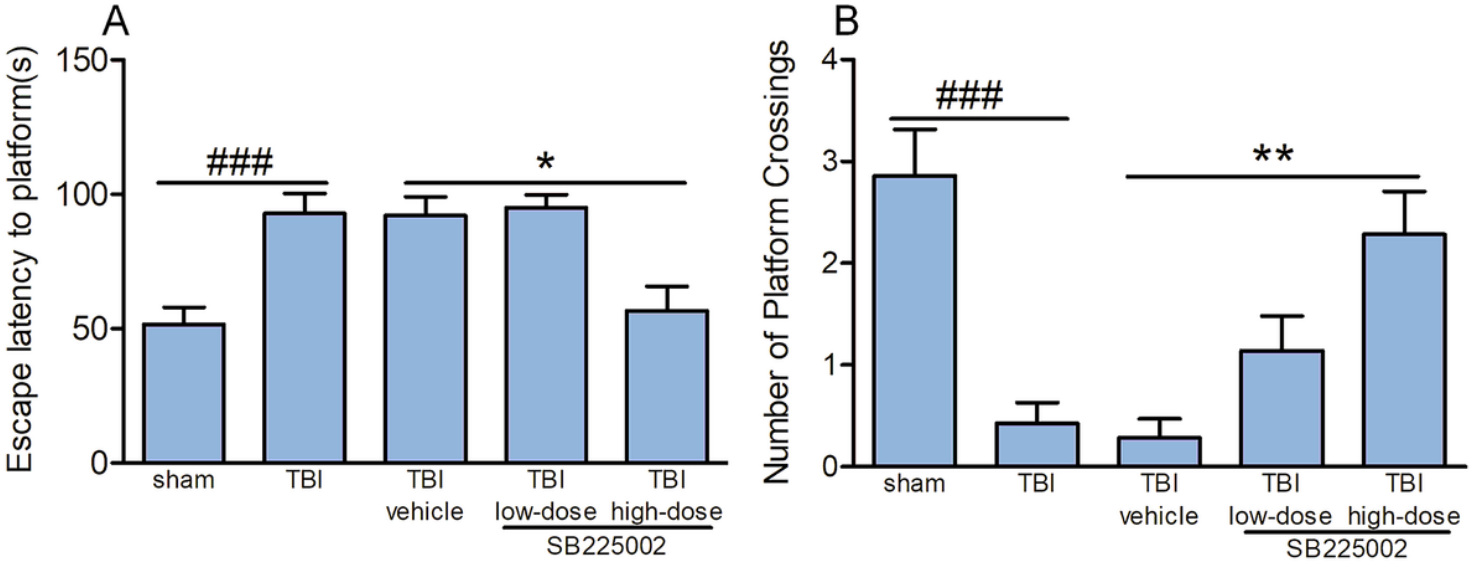

Figure 7

Cognitive function of TBI rats is improved after application of high-dose CXCR2 antagonist SB225002. (A) The escape latency in TBI rats is shortened after high dose of CXCR2 antagonist. (B) The number of platform crossings in TBI rats is increased after high dose of CXCR2 antagonist. Values are expressed as mean ± SEM. **p < 0.01, *p < 0.05, vs. TBI vehicle; ###p < 0.001, vs. sham.

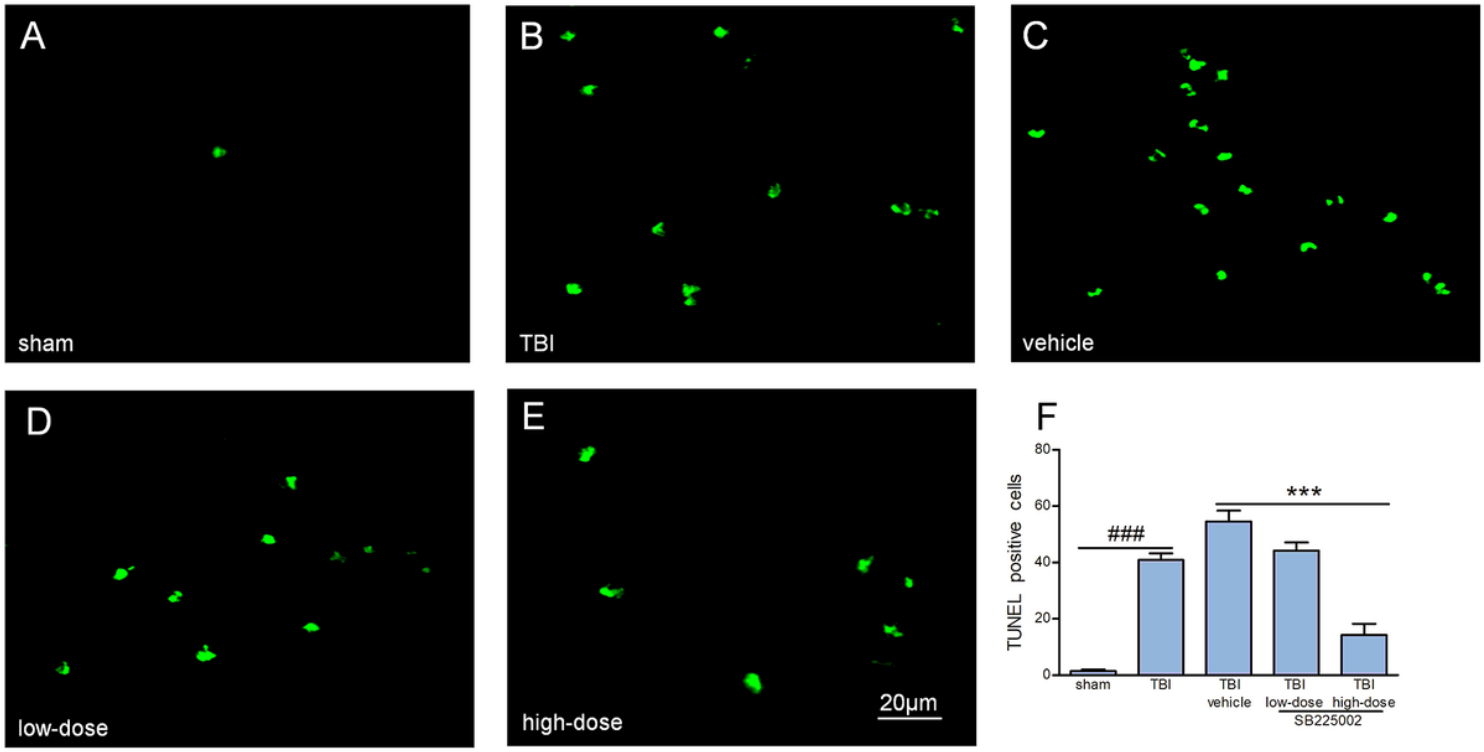

Figure 8

Decreased neuronal apoptosis in TBI rats after application of CXCR2 antagonist SB225002. (A-E) The number of TUNEL-positive cells in the cortex of the injured area 3 days after injury in sham, TBI, TBI vehicle, TBI low dose, and TBI high dose. (F) The number of TUNEL-positive cells in the cortex of TBI rats in the injury area is significantly reduced after application of high dose of CXCR2 antagonist. Values are expressed as mean ± SEM. ***p < 0.001, vs. TBI vehicle; ###p < 0.001, vs. sham.

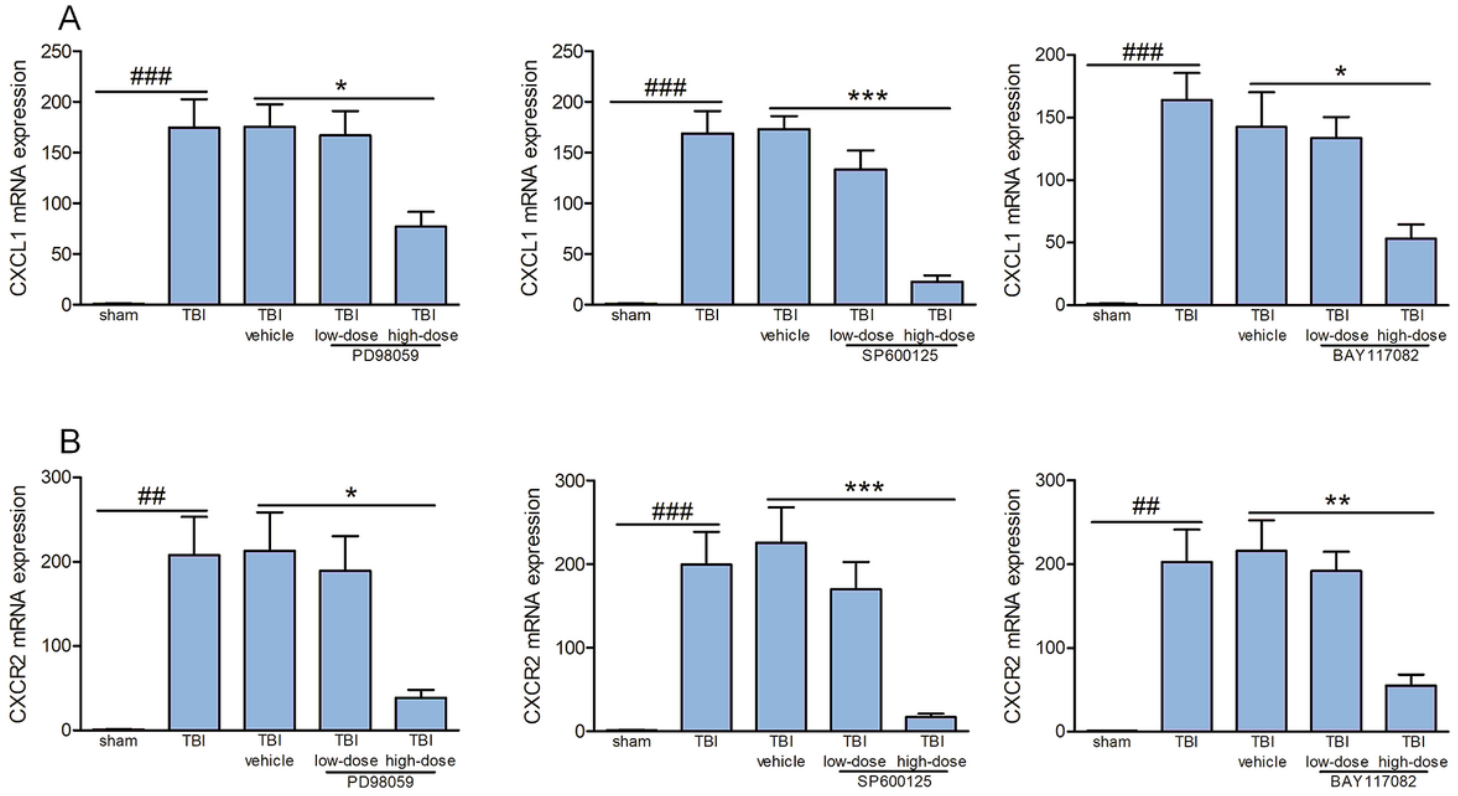

Figure 9

ERK, JNK, and NF-κB inhibitors PD98059, SP600125, and BAY117082 down-regulate CXCL1 and CXCR2 mRNA expression. (A) CXCL1 mRNA expression is decreased 3 days after continuous injection of high doses of ERK, JNK, and NF-κB inhibitors. (B) CXCR2 mRNA expression is decreased 3 days after continuous injection of high doses of ERK, JNK, and NF-κB inhibitors. Values are expressed as mean ± SEM. *** $p < 0.001$, **$p < 0.01$, * $p < 0.05$, vs. TBI vehicle; ###$p < 0.001$, ##$p < 0.01$, vs. sham.

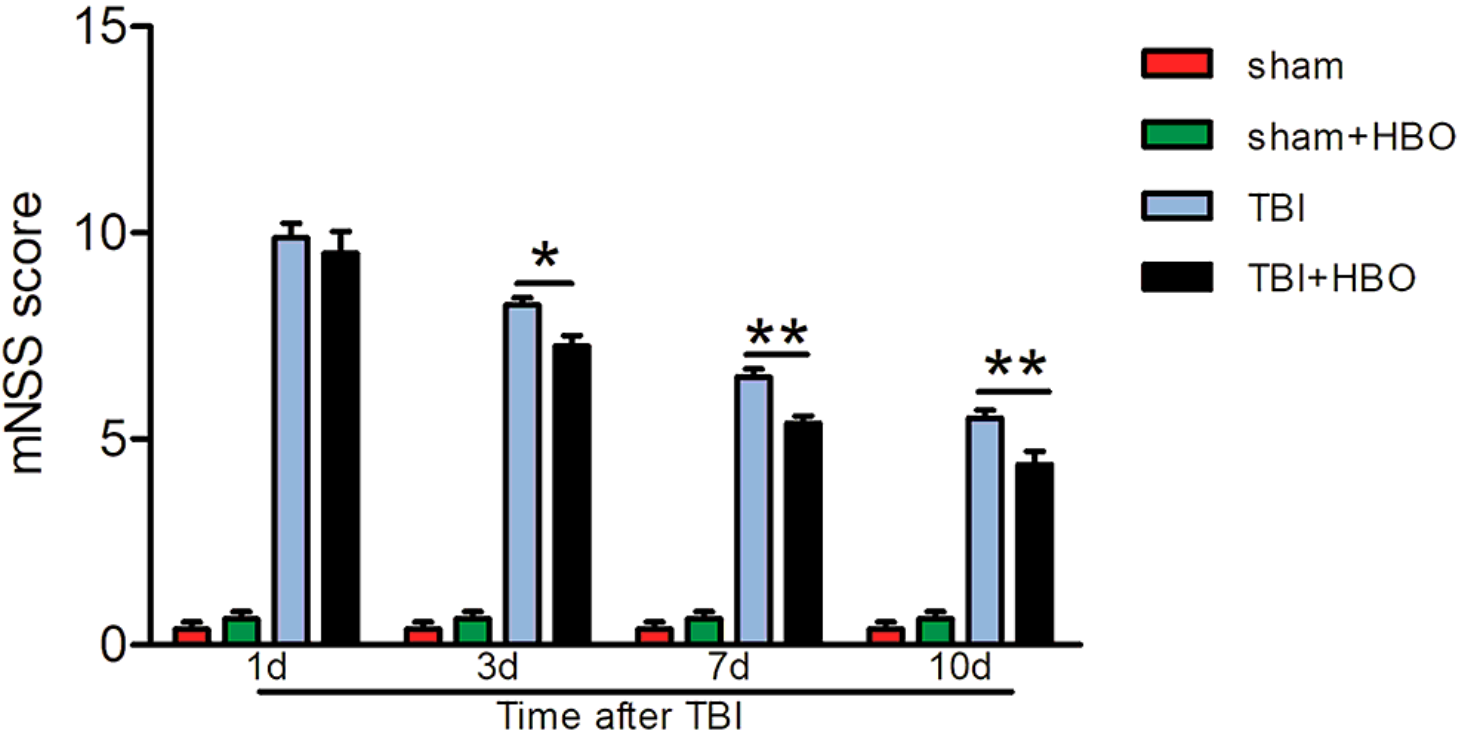

Figure 10

HBO therapy improves neurological function in TBI rats. mNSS scores are lower in after TBI+HBO than TBI alone at 3, 7, and 10 days after TBI. Values are expressed as mean ± SEM. **p < 0.01, *p < 0. 05.

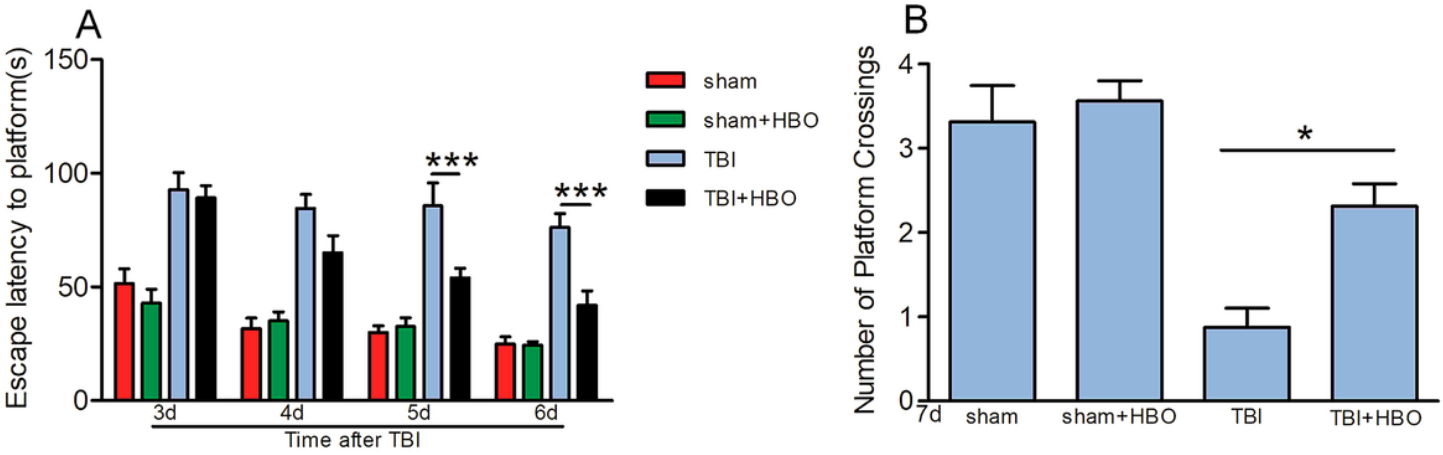

Figure 11

HBO treatment improves cognitive function in TBI rats. (A) In the locomotor navigation test, the escape latency is significantly lower after TBI+HBO than in TBI on days 5 and 6. (B) In the exploration test, the number of platform crossings is higher after TBI+HBO than TBI alone. Values are expressed as mean ± SEM. ***p < 0.001, *p < 0. 05.

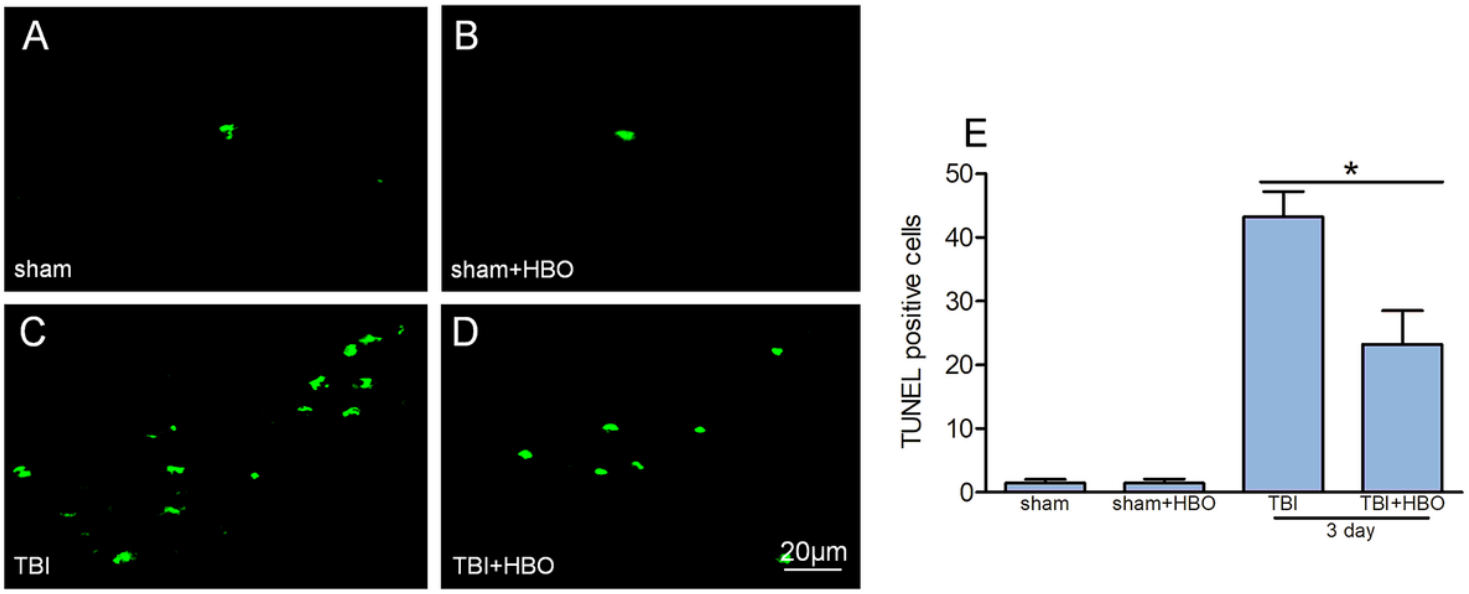

Figure 12

Decreased neuronal apoptosis in TBI rats after HBO treatment. (A-D) The number of TUNEL-positive cells (Bar=20 μm) in the cortex of the injured area 3 days after injury in sham, sham+HBO, TBI and TBI+HBO. (E) The number of TUNEL-positive cells in the cortex of TBI rats in the injury area after HBO treatment is significantly reduced compared to TBI alone. Values are expressed as mean ± SEM. *p < 0. 05.

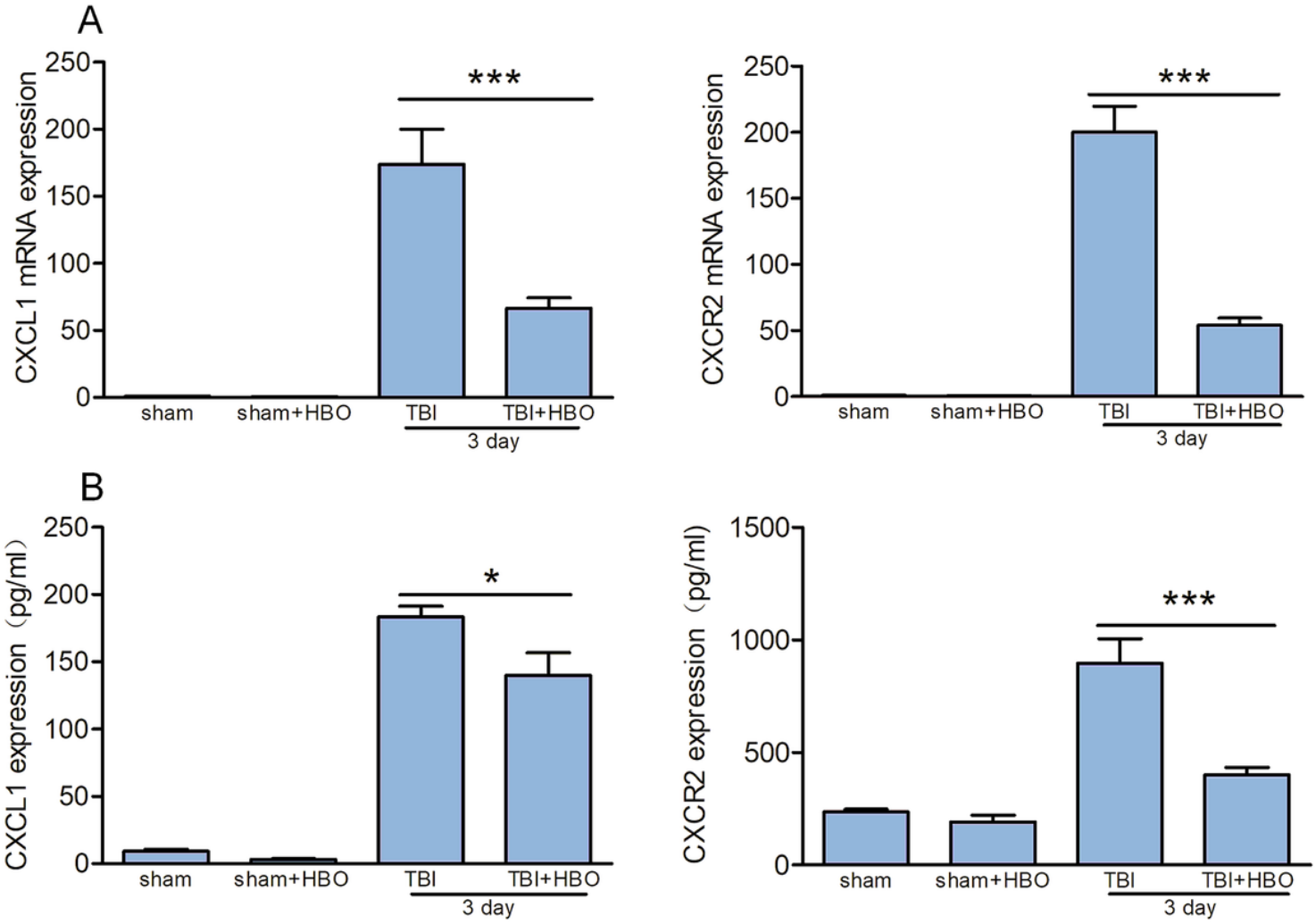

Figure 13

HBO treatment down-regulates mRNA and protein expression of CXCL1, CXCR2. (A) mRNA expression of CXCL1 and CXCR2 decreases after 3 days of HBO treatment. (B) protein expression of CXCL1 and CXCR2 decreases after 3 days of HBO treatment. Values are expressed as mean ± SEM. ***$p < 0.001$, *$p < 0.05$.

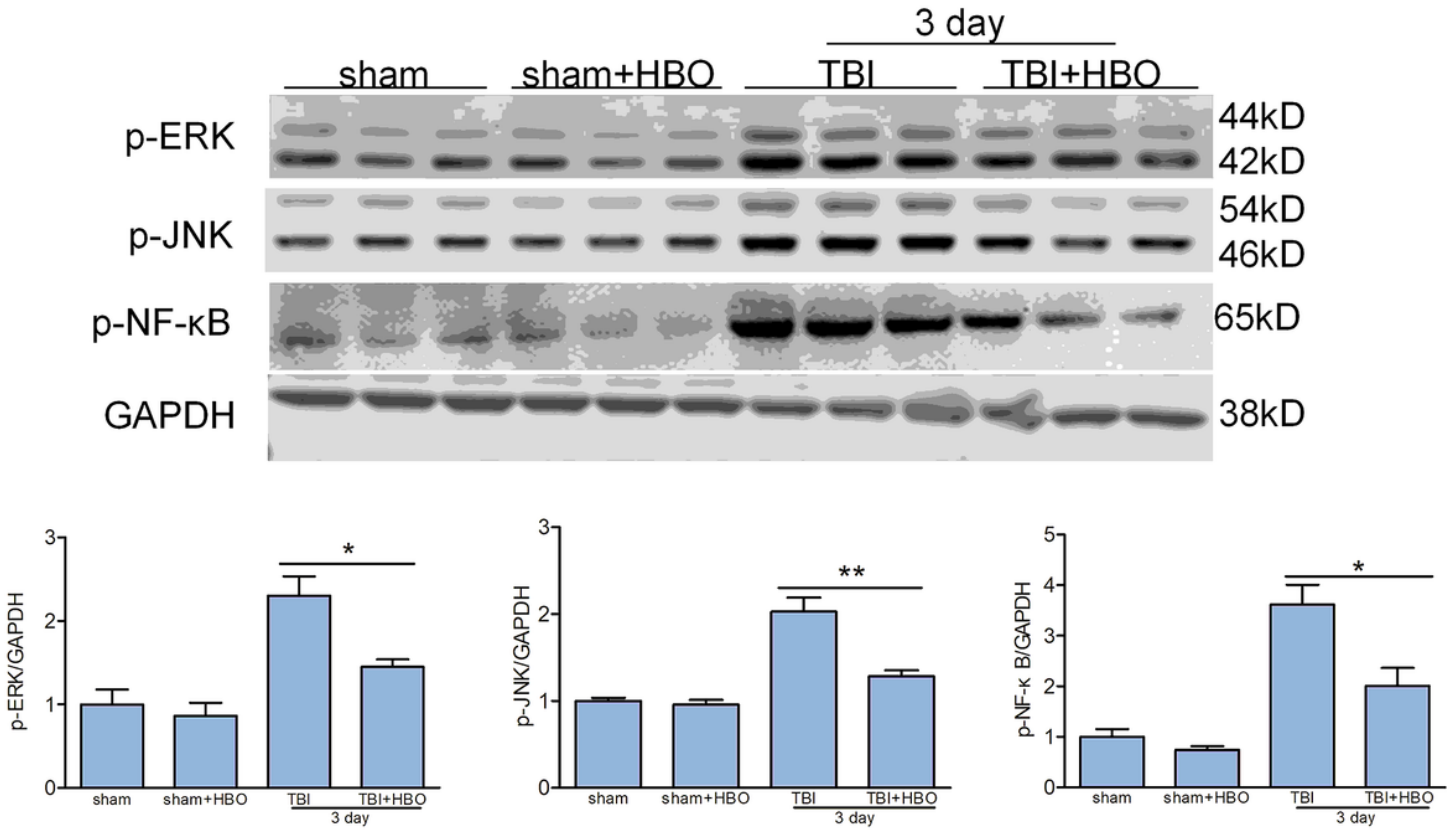

Figure 14

HBO treatment down-regulates expression of ERK, JNK, and NF-κB. p-ERK, p-JNK, and p-NF-κB expression is significantly decreased after continuous HBO treatment for 3 days compared to TBI alone. Values are expressed as mean ± SEM. **p < 0.01; *p < 0.05.